Yttria-Coated FeCo Magnetic Nanoneedles

Nuria O. Núñez,[†] Pedro Tartaj,*[,†] M. Puerto Morales,[†] Pierre Bonville,[‡] and Carlos J. Serna[†]

Instituto de Ciencia de Materiales de Madrid, CSIC, Cantoblanco, 28049, Madrid, Spain and CEA, CE Saclay, Service de Physique de l'État Condensé, 91191 Gif-sur-Yvette, France

Received January 25, 2004. Revised Manuscript Received June 2, 2004

Yttria-coated FeCo nanoneedles with a Co content up to 30 mol % were obtained by thermal reduction of oxyhydroxide precursors. Incorporation of Co and Y elements, with the adequate sequential distribution, to the Fe-based oxyhydroxides was carried out by an oxidation−precipitation method followed by a template method. Special emphasis has been set to correlate the physicochemical characteristics with the magnetic properties of the obtained samples. In this way, Mössbauer and X-ray photoelectron spectroscopy have allowed us to determine that the FeCo metallic core of the particles consists of areas with Fe and Co atoms randomly distributed and also forming clusters. We also established that the improvement in coercivity in metallic particles coated with yttria instead alumina could be associated with the higher degree of thermal protection supplied by yttria. We found that the highest values of coercivity (1550 Oe) are obtained for the yttria-coated FeCo metallic samples with a Co content of 20 mol %. Finally, differences in coercivity between the samples containing different Co content have been associated with both the Co content and microstructure.

Introduction

Nanocrystalline magnetic materials often reveal unique properties that differ from their bulk polycrystalline counterparts. Recent attention in this area comes partly from data storage technology[1] and biotechnology[2] and partly because nanomagnets provide a highly controlled experimental system for studying fundamental phenomena in the area of physical chemistry.[3] Of special interest is the use of nanocrystalline metallic alloys for the storage of digital and analogue signals in the area of advanced flexible media.[4] These media consist of Fe-based needlelike nanoparticles (high anisotropy shape along with improved bit-packing densities) coated with an oxide protecting layer, which are deposited longitudinally on a film.[5]

Ultimately, the magnetic behavior of these materials is closely associated with the crystallochemical characteristics of the particles (mainly particle size distribution, coating homogeneity, and particle microstructure).[4] Therefore, it seems necessary to create new synthetic routes or to develop existing ones in order to obtain more uniform materials in a rather simple way. This will help to generate materials that show better magnetic properties and, importantly, better understand how different factors, e.g., microstructural characteristics, affect the magnetic response of materials.

We have recently shown that the thermal reduction of goethite precursors prepared by a modified carbonate route, which essentially consists of a two-step method in which NaOH and Na_2CO_3 are used as precipitating agents, produces Fe-based alloys with the adequate microstructure and good magnetic properties.[6] In particular, the addition of Co during goethite synthesis and further coating with alumina allowed us to obtain metallic particles with a coercivity of 1160 Oe.[6c] However, by this method only 10 mol % of Co can be incorporated to the system when it is amply reported that in FeCo alloys the highest magnetic moment is obtained for a Co content of 30 mol %.[7] Besides, it has

* To whom correspondence should be addressed. E-mail: ptartaj@icmm.csic.es.

[†] Instituto de Ciencia de Materiales de Madrid.

[‡] Service de Physique de l'État Condensé.

(1) (a) Sun, S.; Murray, C. B.; Weller, D.; Folks, L.; Moser, A. *Science* **2000**, *287*, 1989. (b) Skumryev, V.; Stoyanov, S.; Zhang, Y.; Hadjipanayis, G.; Givord, D.; Nogués, J. *Nature* **2003**, *423*, 850.

(2) (a) Tartaj, P.; González-Carreño, T.; Serna, C. J. *Adv. Mater.* **2001**, *13*, 1620. (b) Dyal, A.; Loos, K.; Noto, M.; Chang, S. W.; Spagnoli, C.; Shafi, K. V. P. M.; Ulman, A.; Cowman, M.; Gross, R. A. *J. Am. Chem. Soc.* **2003**, *125*, 1684. (c) Tartaj, P.; Serna, C. J. *J. Am. Chem. Soc.* **2003**, *125*, 15754. (d) Perez, J. M.; Simeone, F. J.; Saeki, Y.; Josephson, L.; Weissleder, R. *J. Am. Chem. Soc.* **2003**, *125*, 10192. (e) Fan, J.; Lu, J.; Xu, R.; Jiang, R.; Gao, Y. *J. Colloid Interface Sci.* **2003**, *226*, 215. (f) Pankhurst, Q. A.; Connolly, J.; Jones, S. K.; Dobson, J. *J. Phys. D: Appl. Phys.* **2003**, *36*, R137. (g) Tartaj, P.; Morales, M. P.; Veintemillas-Verdaguer, S.; González-Carreño, T.; Serna, C. J. *J. Phys. D*: *Appl. Phys.* **2003**, *36*, 182.

(3) (a) Redl, F. X.; Cho, K.-S.; Murray, C. B.; O'Brien, S. O. *Nature* **2003**, *423*, 968. (b) Tartaj, P.; González-Carreño, T.; Serna, C. J. *J. Phys. Chem. B* **2003**, *107*, 20. (c) Sun, S.; Anders, S.; Thomson, T.; Baglin, J. E. E.; Toney, M. F.; Hamann, H. F.; Murray, C. B.; Terris, B. D. *J. Phys. Chem. B* **2003**, *107*, 5419.

(4) (a) O'Grady, K.; White, R. L.; Grundy, P. *J. Magn. Magn. Mater.* **1998**, *177*−*181*, 886. (b) O'Grady, K.; Laidler, H. *J. Magn. Magn. Mater.* **1999**, *200*, 616.

(5) (a) Sugita, N.; Mackawa, M.; Ohta, Y.; Okinaka, K.; Nagai, N. *IEEE Trans. Magn.* **1995**, *31*, 2854. (b) Onodera, S.; Kondo, H.; Kawana, T. *MRS Bull.* **1996**, *21*, 35. (c) Hisano, S.; Saito, K.; Aizawa, S.; Sano, K.; Matsumoto, K.; Murata, K. U.S. Patent No. 5591535, 1997. (d) Hisano, S.; Saito, K. *J. Magn. Magn. Mater.* **1998**, *190*, 371.

(6) (a) Núñez, N. O.; Morales, M. P.; Tartaj, P.; Serna, C. J. *J. Mater. Chem.* **2000**, *10*, 2561. (b) Núñez, N. O.; Pozas, R.; Morales, M. P.; Tartaj, P.; Bonville, P.; Caballero, A.; González-Elipe, A. R.; Ocaña, M.; Serna, C. J. *Chem. Mater.* **2003**, *15*, 951. (c) Núñez, N. O.; Tartaj, P.; Morales, M. P.; Pozas, R.; Ocaña, M.; Serna, C. J. *Chem. Mater.* **2003**, *15*, 3558.

(7) (a) Bardos, D. I. *J. Appl. Phys.* **1969**, *40*, 1371. (b) Terseff, J.; Falikov, L. M. *Phys. Rev. B* **1982**, *25*, 4937. (c) Victora, R. H.; Falikov, L. M. *Phys. Rev. B* **1984**, *30*, 259.

10.1021/cm049860v CCC: $27.50
Published on Web 07/17/2004

been recently pointed out that yttria instead alumina coatings are ideal protective agents for the most advanced metal particulate recording media.[5c]

In this article we report the synthesis and characterization of needlelike yttria-coated FeCo nanoparticles starting from needlelike YCo−FeOOH nanoparticles. The synthetic method here reported combines the superior advantages of the synthesis of needlelike particles by a modified carbonate route, such as high axial ratio, adequate particle size, and production rate, with the unique characteristics of the electrostatically induced self-assembly methods, i.e., template methods, that under particular conditions (mainly pH and salt and solid concentrations) can produce homogeneous coatings with different spatial arrangements.[8] In addition to the preparation, we characterized the metallic particles in terms of morphology and chemical and phase composition. We also carried out a detailed magnetic characterization to try to establish the reason for which the use of yttria instead alumina coatings leads to metallic particles with higher coercivity. Finally, to determine the role of yttria in combination with Co in improving the coercivity value of the Fe alloys, we correlated the physicochemical characteristics of the samples with their magnetic behavior.

Experimental Section

Materials. Analytical-grade reagents ferrous sulfate $Fe(SO_4)\cdot 7H_2O$ (Fluka), cobalt nitrate $Co(NO_3)_2\cdot 6H_2O$ (Aldrich), yttrium nitrate $Y(NO_3)_3\cdot 6H_2O$ (Aldrich), aluminum nitrate $Al(NO_3)_3\cdot 9H_2O$ (Aldrich), sodium carbonate Na_2CO_3 (Carlo Erba), and sodium hydroxide NaOH (Aldrich) and doubly distilled water previously deaerated with N_2 were used in all experiments.

Sample Preparation. Co−goethite particles with needlelike morphology with rather uniform size dispersion were obtained by oxidation−precipitation of $FeSO_4$ and $Co(NO_3)_3$ solutions following a method described earlier.[6] It essentially consists of the sequential oxidation−precipitation of $FeSO_4$ and $Co(NO_3)_2$ aqueous solutions (0.1 M total salt concentration) first with NaOH (0.35 OH/(Fe+Co) equivalent ratio) and then with Na_2CO_3 (1.5 CO_3^{2-}/(Fe+Co) equivalent ratio) at 40 °C. By this method only 10 mol % of Co can be incorporated to the system because higher amounts promote the formation of other crystalline phases apart from the needlelike goethite nanoparticles (from now on these particles are referred as Co−goethite).

We developed a simple and versatile method to increase the Co content and produce particles with a surface enriched in Y_2O_3. The method is based on the electrostatically induced adsorption of nanoparticles with opposite surface charge density onto the needlelike Co−goethite particles. The coating process involved, first, the dissolution in water (previously deaerated with N_2 to avoid Co(II) oxidation) of $Co(NO_3)_2$ and $Y(NO_3)_3$ at a pH of ∼3 in the desired proportions followed by the addition of KOH to a pH of ∼12. Then the Co−goethite particles (10 g L^{-1}) were homogeneously suspended in this solution. Immediately after, CO_2 was bubbled into the slurry to slowly lower the pH to a value of 10.5, where the pH was kept constant for 15 min, and then to a pH of 9.5. This sequence is not arbitrary but based on the different values of surface charge density at selected pH regions of the Co−goethite particles and the generated Co and Y species present in solution.

To prove the beneficial effect of replacing alumina by yttria coatings on the magnetic properties of the metallic particles and, if beneficial, try to explain the reason for this beneficial effect, Co−goethite particles were coated with alumina (from now on these particles are referred as FeCo10Al) instead of yttria following a procedure described earlier.[6c]

Thermal Reduction. For reduction, the oxyhydroxide precursors were dehydrated in air at different temperatures for 2 h and then reduced at 400 °C in a H_2 stream of 40 L h^{-1} for 4 h. The samples were then cooled to room temperature under a hydrogen atmosphere. Finally, nitrogen gas was blown into a flask containing ethanol, and the resulting stream was passed through the sample (∼1 h) to passivate the iron particle surface in a controlled way. Without passivation, samples could rapidly oxidize upon exposure to air.

Characterization Techniques. Phase identification was carried out by X-ray diffraction (XRD) in a Philips PW1710 using Cu Kα radiation. Particle size and shape of the samples were examined by transmission electron microscopy (TEM, JEOL 2000 FX). The mean length and width and the standard deviation associated with these two parameters were evaluated from the electron micrographs by counting ca. 100 particles. The mean and standard deviation values associated with the axial ratio were evaluated from the length/width ratios obtained for each particle. The cobalt content in the goethite samples was determined by plasma emission (ICP, Perkin-Elmer 5500). For this analysis, 100 mg of powder was first dissolved with concentrated HCl and then diluted with doubly distilled water. Chemical analyses at the particle level of samples were done with an energy dispersive spectrometry analyzer (EDX, Oxford Link QX 2000) integrated in the TEM.

Specific surface area measurements of samples (BET method) were carried out in a Micromeritics Flowsorb 2300 using N_2 as adsorbate. X-ray photoelectron spectra (XPS) were recorded in a VG Escalab 220 using a Mg Kα excitation source. Isoelectric point values were experimentally obtained by measuring the electrophoretic mobility as a function of pH with a Coulter Delsa 440.

^{57}Fe Mössbauer absorption spectroscopy was used to characterize the final iron particles. The spectra were recorded with a maximum velocity of 10 mm s^{-1} at room temperature and 4.2 K with a ^{57}Co:Rh source. The hyperfine field and the isomer shift were obtained from the spectra by a standard procedure, using Lorentzian-shaped lines. The isomer shift value is given relative to that of α-Fe.

Magnetic characterization of the samples was carried out in a vibrating sample magnetometer (VSM, MLVSM9 MagLab 9 T of Oxford Instrument). Hysteresis loops were recorded at 298 K after applying a saturating field of 3 T. The saturation magnetization (Ms) and coercivity (Hc) were obtained from the loops for each sample. The Ms values were evaluated by extrapolating to infinite field the experimental results obtained in the high-field range where the magnetization linearly increases with $1/H$.

Results and Discussion

Coating Mechanism and Characterization of Oxyhydroxide Precursors. The search for an ideal method of coating must be based on some premises: (1) coating homogeneity, (2) high production rate (the coating process, if possible, must be carried out in a single experiment), and (3) adequate coating microstructure. Regarding the third premise, in our case the ideal spatial arrangement should consist of a shell-in-shell structure. This shell-in-shell structure must consist of an inner surface layer of species containing cobalt surrounded by an outer layer of species containing yttrium. In this way, during the necessary thermal reduction process carried out to obtain the metallic particles, the Co could diffuse within the Fe metallic core (Fe and Co form metallic alloys in all range of compositions). Thus, we can expect the micro-

(8) (a) Caruso, F. *Adv. Mater.* **2001**, *13*, 11. (b) Tartaj, P. *ChemPhysChem* **2003**, *4*, 1371.

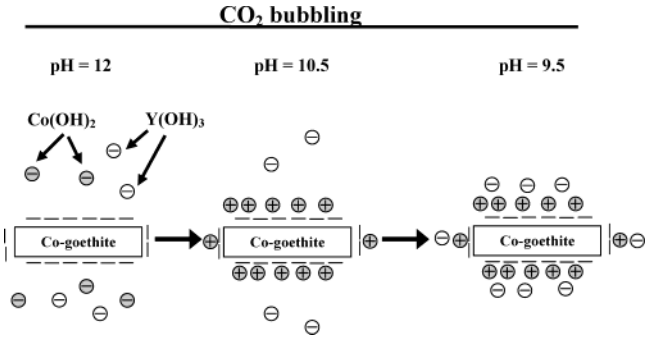

Figure 1. Schematic representation of the electrostatically induced self-assembly process that leads first to the adsorption of Co(II) hydroxide onto the needlelike templates and finally to the adsorption of Y(III) hydroxide.

structure of the final metallic particles to be composed of an FeCo metallic core protected with a outer shell of yttria.

As mentioned in the Experimental Section, the suspensions containing the Co−goethite particles and the Co(II) and Y(III) species in solution were brought to a pH of 12. At this pH, we expect the formation of Co(II) and Y(III) hydroxides.[9] Co(II) and Y(III) hydroxides have isoelectric point (IEP) values of 11 and 9, respectively, while Co-doped goethite samples have an IEP value of 8.[10] Thus, at a pH of 12 all species have negative values for the surface charge density, and therefore, no adsorption is expected to take place. Besides, at this pH, the high value of the Co−goethite surface charge density favors the formation of stable suspensions. At a pH of 10.5, the surface charge density of the Co(II) hydroxide acquires positive values (pH region below the IEP), and therefore, these species can be adsorbed on the negatively charged goethite surface (the 15 min residence time at this pH was found to be sufficient for the Co(II) hydroxide to be adsorbed). The cobalt coating induces a reversal of the surface charge of the needlelike Co−goethite particles from negative to positive values, and therefore, the yttrium hydroxide that remains negatively charged can be subsequently adsorbed in the pH range between 10.5 and 9 (pH values above the IEP of yttrium hydroxide). A schematic representation of the sequential adsorption mechanism is displayed in Figure 1, and the microstructure of the resulting particles is displayed in Figure 2. We can observe that combination of the synthesis by a modified carbonate route with the template method allowed the formation of uniform layers of cobalt and yttrium hydroxides around needlelike goethite nanoparticles (Figure 2).

According to chemical analysis carried out by ICP, the amount of Y and Co found in the solids was equal to that initially added for the coating process. In particular, the amount of Y added with this method was set to a value of 3 mol %. This value was found to be the minimum amount of this element that helps to preserve the needlelike morphology during the reduction. Higher amounts of Y also preserve the needlelike shape but also

(9) Burriel, F.; Lucena, F.; Arribas, S.; Hernández, J. In *Química Analítica Cualitativa*; Paraninfo: 1989.

(10) The isoelectric points for Co(II) and Y(III) hydroxides were obtained from the following reference: Parks, G. *Chem. Rev.* **1965**, *39*, 177. Isoelectric points for the Co-doped goethite particles were experimentally obtained by measuring the electrophoretic mobility as a function of pH with a Coulter Delsa 440.

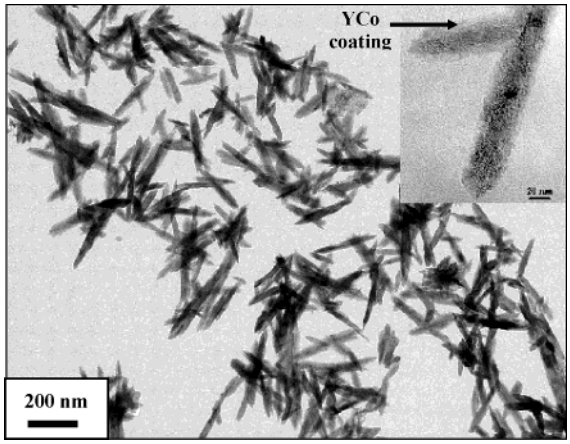

Figure 2. Typical microstructure of the needlelike goethite particles coated with a homogeneous layer containing Co(II) and Y(III) hydroxides.

produce an increase in the content of undesired nonmagnetic phases. Meanwhile, the amount of Co added by this method was varied to produce samples with a total content of 10 (no cobalt added during the coating, sample FeCo10Y), 20 (10 mol % of cobalt added during the coating, FeCo20Y), and 30 mol % (20 mol % of cobalt added during the coating, FeCo30Y). As mentioned above, the highest magnetic moment in FeCo alloys is obtained for a Co content of 30 mol %, and therefore, the amount of this element added to the system was restricted to an upper limit of 30 mol %. Logically, for the sample in which no cobalt was added during the coating (FeCo10Y), the pH was brought directly from 12 to 8.5 to induce adsorption of yttrium hydroxide on the needlelike Co-doped goethite particles. At this pH the surface of goethite remains negatively charged while the surface of the ytrrium hydroxide nanoparticles has already attained positive values. It is worth mentioning that samples FeCo10Y and FeCo10Al (see Experimental Section and ref 6c for details of its preparation) only differ in the nature of the coating (yttria versus alumina) and so can be used to determine which of the two protective oxides is more beneficial for the magnetic properties.

Chemical analyses carried out by EDX at the particle level in samples FeCo10Y, FeCo20Y, and FeCo30Y showed a similar composition to that of the overall solid, which indicates that all Y and Co is found deposited on the needlelike particles. In accordance with the presence of an outer layer containing yttrium hydroxide species (i.e., sequential mechanism of adsorption), the IEP of all samples, irrespective of the cobalt content, was 8.9, similar to that of $Y(OH)_3$ (Figure 3). Additional confirmation of the sequential adsorption mechanism was obtained from XPS. For example, for the sample containing a total content in cobalt of 30 mol % (20 mol % added during the coating) and 3 mol % in yttrium, the Y/(Co + Y) molar ratio obtained on the surface was 45%, while the expected value for an adsorption process following a nonsequential mechanism should be around 13% (3/(20 + 3)).

Formation of Metallic Particles. Starting from oxyhydroxide precursors, we can expect that during the thermal reduction process that leads to the formation of metallic particles some internal porosity can be developed in the particles as a consequence of the loss

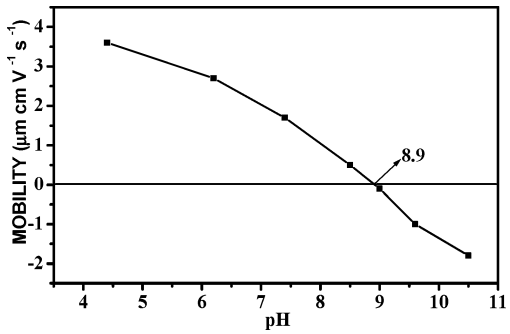

Figure 3. Typical electrophoretic mobility curve as a function of pH for the needlelike goethite particles coated with a homogeneous layer containing Co(II) and Y(III) hydroxides.

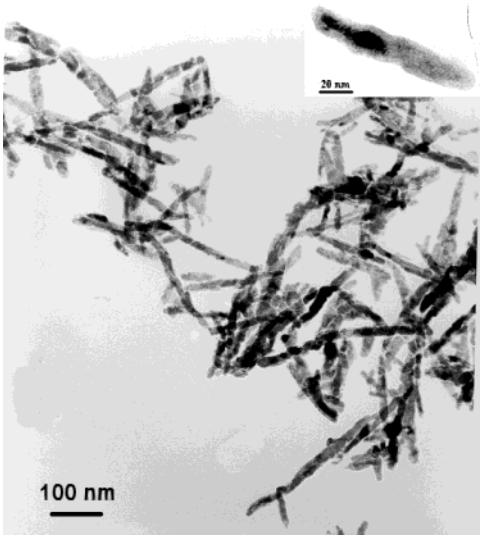

Figure 4. Typical microstructure of the needlelike FeCo metallic particles showing a central metallic core surrounded by an outer layer containing (as it is explained in the text) oxide species.

of OH. Porosity inside particles can harm the magnetic properties exhibited by the final metallic particles, and so, prior to the thermal reduction, the oxyhydroxide precursors were thermally treated in air. Heating in air first leads to the dehydration of the oxyhydroxide precursors and then at a higher temperature promotes a decrease in internal porosity. Logically, because the primary factor that controls the value of coercivity in needlelike particles is shape anisotropy, the heating must be restricted to temperatures in which the needlelike shape is preserved. For particles coated with yttria, we found the maximum temperature to be 600 °C. It is worth noting that this temperature is 200 °C higher than that previously found for particles coated with alumina (400 °C).[6c] Thus, the use of yttria instead alumina allows one to increase the annealing temperature from 400 to 600 °C (porosity reduction more effective).

After reduction, the samples consisted of needlelike FeCo metallic nanoparticles (XRD only showed diffraction peaks due to α-Fe) with a mean length of 170 ± 40 nm and a mean width of 20 ± 5 nm (axial ratio of 8 ± 2; Figure 4). Chemical analyses carried out by EDX at the particle level showed a similar composition to that of the overall solid, which indicates that thermal treatment produces no segregation of phases. XRD cannot discard the presence of other phases such as the iron oxide spinel usually produced during the passivation process of metallic iron.[11] This phase normally appears in the form of nanocrystals about 2 nm in size (with a grain size lower than ∼2 nm, diffraction effects are diffuse and close to the background noise) that combined with its low content could be the reason for its possible absence in the XRD patterns.

XPS of samples were registered to determine the possible presence of an iron oxide passivation layer and also to determine whether thermal treatment was sufficient to induce diffusion of Co within the Fe matrix. XPS (Figure 5) clearly evidenced the presence of an iron oxide passivation layer containing Co(II) cations. The spectra were characterized by two broad main peaks at 782.3 and 798.2 eV due to Co 2p and two strong associated satellites located at the high binding energy side of the main peaks. The position and intensity of these peaks are typical of the presence of Co(II). [12] The spectrum also shows bands at 711.5 and 725.1 eV associated with the presence of iron oxide and a band at 157.5 eV associated with yttrium oxide.[13] Quantitative analyses carried out by XPS showed that the Co/(Co+Fe) molar content on the surface was similar to the average obtained for the solid, which indicates that thermal treatment induces the Co-diffusion inside the Fe matrix. XPS also showed an increase in the amount of Y_2O_3 present on the surface, which is consistent with the role of this compound on preventing the interparticle sintering.

Mössbauer spectroscopy (Figure 6) was used for identification and quantification of the iron oxide present on samples and also to elucidate the Co distribution within the Fe core. The spectrum at 4.2K of sample FeCo20Y, chosen as representative, contains three sextets. One sextet with an isomer shift of 0.40 mm s^{-1} and a hyperfine field of 50.0 T can be attributed to the presence of an iron oxide spinel containing, as suggested by XPS, Co(II) cations (cobalt ferrite). This phase represents in all samples 50 wt % of the total, which corresponds to a thickness layer between 2 and 5 nm, which is of the size suggested by TEM (Figure 4). In accordance with the presence of an iron oxide passivation layer of about 2−5 nm, the Mössbauer spectra registered at room temperature (Figure 6) shows a broad quadrupolar doublet (superparamagnetic behavior) typical of iron oxide spinels having these crystallite sizes.[14,15] The fact that the passivation layer was independent of the cobalt content indicates that its presence is primarily controlled by the particle size and the thickness of the Y_2O_3 coating.

The Mössbauer spectra at 4.2 K (Figure 6) show two more sextets (also visible at room temperature) with an

(11) Theil Kuhn, L.; Bojsen, A.; Timmerman, L.; Meedom-Nielsen, M.; Mørup, S. *J. Phys.: Condens. Matter* **2002**, *14*, 13551.
(12) (a) Kim, K. S. *Phys. Rev. B* **1975**, *11*, 2177. (b) Tyuliev, G.; Angelov, S. *Appl. Surf. Sci.* **1988**, *32*, 381. (c) Van, J.; Wieland, J. L.; Kuiper, P.; Scwatzky, G. A.; De Groot, F. M. F.; Turner, T. S. *Phys. Rev. B* **1991**, *44*, 6090. (d) Jiménez, V. M.;, Espinos, J. P.; González-Elipe, A. R. *Surf. Interface Anal.* **1998**, *26*, 62.
(13) Wagner, C. D.; Riggs, W. M.; Davis, L. E.; Moulder, G. E.; Muilenberg, G. E. *Handbook of X-Ray Photoelectron Spectroscopy*; Perkin-Elmer, MN, 1979.
(14) Mørup, S.; Bødker, F.; Hendriksen, P. V.; Linderoth, S. *Phys. Rev. B* **1995**, *52*, 287.
(15) Martinez, B.; Roig, A.; Molins, E.; González-Carreño, T.; Serna, C. J. *J. Appl. Phys.* **1998**, *83*, 3256.

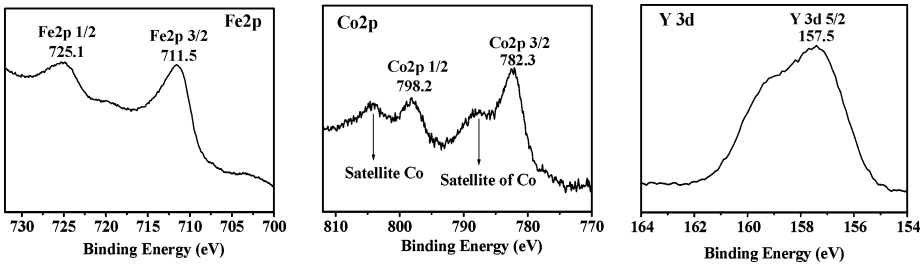

Figure 5. XPS diagrams of sample FeCo20Y (chosen as representative).

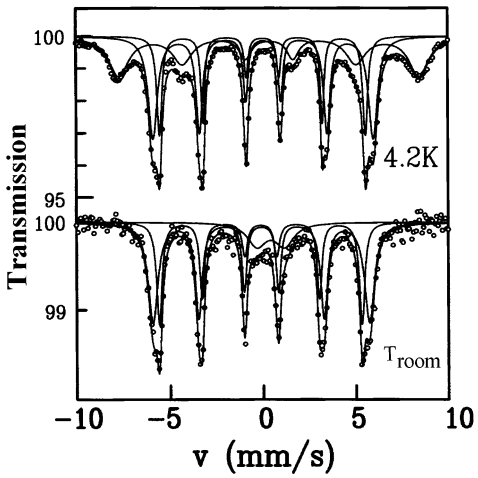

Figure 6. Mössbauer spectrum of sample FeCo20Y (chosen as representative) registered at room temperature and 4.2 K. Similar Mössbauer spectra were observed for the other two samples.

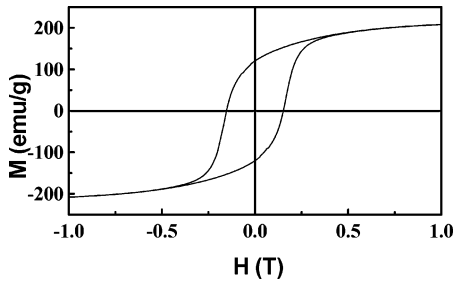

Figure 7. Magnetic hysteresis loop of sample FeCo20Y (chosen as representative) registered at RT. Similar hysteresis loops were observed for the other two samples.

isomer shift of 0.0 mm s^{-1} and hyperfine fields of 36.65(10) and 34.25(10) T. These hyperfine field values are larger than that of pure metallic iron (34 T at 4.2 K) and correspond to Fe−Co alloys. Here it is worth noting that if the distribution of Fe and Co atoms inside particles is inhomogeneous (there is some kind of aggregation of Fe atoms and therefore of Co atoms), the hyperfine field value does not necessarily reflect the average composition of the particle (in particular, the obtained value should be close to the one of pure metallic Fe). Indeed, it has been shown[16] that the hyperfine field H_{hf} at the ^{57}Fe nucleus increases with Co concentration c, for $c < 0.2$, according to the linear law: $H_{hf}(c) = H_{hf}(0)(1 + 0.5c)$. The sextet with hyperfine field 36.65 T at 4.2 K (33 wt %) corresponds to an FeCo alloy with a Co content of ∼16 mol %, similar to the average content of the entire solid. The other sextet (17 wt %) corresponds to an FeCo alloy with a Co content of ∼2 mol %. This result suggests that in the metallic core regions with Co-poor Fe alloy and regions with Co-rich Fe alloy coexist. It is important to mention that this particular distribution is independent of the Co content in the samples and thus independent of the way Co was added to the samples. Alternatively, one could speculate that the sextet with the lowest hyperfine field could be associated with the FeCo atoms located at the surface (close to the passivation layer) since, as previously observed in Fe nanocrystals,[17] atoms located at the interface are expected to have hyperfine field values different from those located in the bulk. However, these signals normally appear fitted with a distribution of hyperfine fields reflecting the intrinsic disorder of the surfaces.

Magnetic Characterization. Hysteresis loops registered at room temperature (Figure 7) clearly showed that the samples exhibited ferromagnetic characteristics including saturation magnetization (Ms) and high coercivity (Hc).

To prove the beneficial effect of replacing alumina by yttria coatings on the magnetic properties of the metallic particles and, if beneficial, try to explain the reason for this beneficial effect, the coercivity values of samples FeCo10Y and FeCo10Al were compared. Sample FeCo10Y has a coercivity of 1380 Oe, while as mentioned above a sample FeCo10Al has a coercivity of 1160 Oe.[6c] This difference in coercivity values could be associated with the different degree of internal porosity that the two samples present prior to thermal reduction treatment. In particular, the samples with the yttria coating have a lower specific surface area determined by the BET method (∼ 30 m^2 g^{-1}) than those samples containing alumina coatings (∼60 m^2 g^{-1}). This result is, of course, a consequence of the different thermal treatment of the precursors. As mentioned above, the oxyhydroxide precursors containing the yttria coatings were heated at 600 °C while the oxyhydroxide precursors containing alumina were heated at 400 °C. Supporting this interpretation, a sample similar to FeCo10Y but heated only at 400 °C prior to thermal reduction (specific surface area of ∼60 m^2 g^{-1}) has a coercivity of 1090 Oe.[18]

Once established the beneficial effect of replacing alumina by yttria coatings, we compared the magnetic behavior of the yttria-coated metallic particles contain-

(16) Vincze, I.; Campbell, I. A.; Meyer, A. *J. Solid State Commun.* **1974**, 15, 1495.

(17) Del Bianco, L.; Hernando, A.; Bonetti, E.; Navarro, E. *Phys. Rev. B* **1997**, *56*, 8894.

(18) The slight differences in coercivity between this sample and the sample coated with alumina could be associated with slight differences in axial ratio.

ing different amounts of Co. Saturation magnetization values normalized to the metallic content increased slightly with Co content (Ms values for samples FeCo10Y, FeCo20Y, and FeCo30Y were 215, 225, and 230 emu/g, respectively). This result can be explained in terms of the highest magnetic moment of the FeCo alloys containing an amount of cobalt close to 30 mol %. The normalized Ms values are similar to that of the FeCo bulk, which is not surprising for Fe-based metallic particles of about these sizes where surface effects can be neglected.[19,20]

In needlelike particles, the anisotropy field is dominated by shape anisotropy, which is not only a function of the axial ratio but also of the square of Ms.[21] In our samples we could discard an enhancement of anisotropy at room temperature associated with the presence of the Co−ferrite surface layer because according to Mössbauer this phase was superparamagnetic. Therefore, in our samples, in which the axial ratio is similar (∼8), we could expect the particle having the highest Ms value (sample FeCo30Y) to also have the highest Hc value. However, the values of Hc did not follow the expected tendency with Co content. The highest value (1530 Oe) was obtained for sample FeCo20Y, while the lowest value (1380 Oe) was obtained for the sample with the lowest Co content (FeCo10Y), and the sample with the highest Co content (FeCo30Y) has an intermediate Hc of 1470 Oe. Since the difference in Ms values between samples FeCo20Y and FeCo30Y is only about 2%, slight differences in the internal microstructure could be claimed as being responsible for the highest coercivity value manifested by sample FeCo20Y despite having a lower Ms value.

Conclusions

We have shown that thermal reduction of needlelike YCo−goethite particles, prepared by combination of a double-oxidation method with an electrostatically induced self-assembly method, can produce needlelike FeCo metallic particles with adequate magnetic properties. We observed that the use of yttria as a protective agent has allowed the dehydration temperature of the oxyhydroxides to increase, decreasing the porosity of samples and so improving the magnetic properties of the final metallic particles. We determined that in the metallic core regions with Fe and Co atoms randomly distributed and regions with Fe and Co atoms not randomly distributed (forming clusters) coexist. We found that the highest value of coercivity (1550 Oe) is obtained for samples containing a Co content of 20 mol % and that the decrease in coercivity of samples containing higher and lower amounts of Co could be associated with differences in saturation magnetization values and internal microstructure.

Acknowledgment. N.O.N. thanks a grant from AECI. Financial support from CICYT (MAT2002-04001-C02) and the “Acciones Integradas” program HF20020123 are also gratefully acknowledged. P.T. acknowledges the financial support from the Ramon y Cajal program.

CM049860V

(19) Bødker, F.; Mørup, S.; Linderoth, S. *Phys. Rev. Lett.* **1994**, *72*, 282.
(20) Bonetti, E.; Del Bianco, L.; Fiorani, D.; Rinaldi, D.; Caciuffo, R.; Hernando, A. *Phys. Rev. Lett.* **1999**, *83*, 2829.
(21) Cullity, B. D. *Introduction to Magnetic Materials*; Addison-Wesley: CA, 1972.